



<i>Publication Year</i>	2020
<i>Acceptance in OA</i>	2022-02-10T15:54:36Z
<i>Title</i>	Preliminary Analysis of the Effects of the Ground Plane on the Element Patterns of SKA1-Low
<i>Authors</i>	BOLLI, Pietro, Bercigli M., DI NINNI, PAOLA, Labate M.G., Virone G.
<i>Publisher's version (DOI)</i>	10.23919/EuCAP48036.2020.9135350
<i>Handle</i>	http://hdl.handle.net/20.500.12386/31381

Preliminary Analysis of the Effects of the Ground Plane on the Element Patterns of SKA1-Low

Pietro Bolli¹, Mirko Bercigli², Paola Di Ninni¹, Maria Grazia Labate³, Giuseppe Virone⁴

¹ Astrophysical Observatory of Arcetri, INAF, Florence, Italy, pbolli@arcetri.inaf.it

² Ingegneria dei Sistemi, Pisa, Italy

³ Square Kilometre Array Organization, Lower Withington, UK

⁴ Institute of Electronics, Computer and Telecommunication Engineering, CNR, Turin, Italy

Abstract—Each station of the SKA1-Low radio telescope is composed by 256 dual-polarized log-periodic antennas deployed over a metallic ground plane with 42 m diameter. This station is usually modelled in EM simulators by considering an infinite ground plane, which drastically reduces the computational time. This contribution shows that a finite ground plane can bring to quite significant differences in some embedded element patterns with respect to the infinite ground plane case. Furthermore, we show the impact on the antenna pattern of different dielectric media surrounding the finite ground plane. For instance, at 50 MHz the maximum of the antenna gain decreases by 5% for the terrain with 10% moisture level.

Index Terms—Low-frequency aperture array radio telescope, Square Kilometer Array.

I. INTRODUCTION

The most ambitious project of radio astronomy ever, the Square Kilometer Array (SKA), is now approaching to the construction phase, the System Critical Design Review (CDR) being planned for December 2019. The phase 1 low-frequency instrument of SKA (SKA1-Low) will operate between 50 and 350 MHz and is based on an aperture array with log-periodic dual-polarized antennas distributed in 512 stations spread in the Murchison region in Western Australia [1]. In the last years, an intensive and accurate EM modelling process has been conducted to predict the performance of SKA1-Low against the scientific requirements. Bearing in mind that a full-wave analysis of one station including mutual coupling effects would require running time of more than one week for each frequency point, some approximations in the model become necessary. One of them is on the ground plane located under the antennas, which is usually treated with infinite size and composed by a perfect electric conductor (pec). Therefore, diffractions from the edge of the finite ground plane as well as effects from the dielectric terrain have been so far neglected. In this contribution, we partially fill this gap with a preliminary analysis on the perturbation to the antenna patterns due to a more realistic modelling of the ground plane and of the terrain.

II. STATION OF SKA1-Low

An SKA1-Low station is an aperture array composed of 256 log-periodic dual-polarized antennas, randomly distributed within a circular area having a maximum distance between the antenna centers of 38 m, whose signals are combined together in order to form one or more station beams. The antennas are placed over a ground plane, which cover at least a circular area of 42 m as diameter. The ground plane is made of sheets of steel wire reinforcing mesh having dimensions such to act as an electromagnetic reflector at the overall frequency range. Dimensions of the square mesh are 50 x 50 mm with 4 mm diameter of the wires (see Fig. 1).

Two Low-Noise Amplifiers (LNAs) (one for each polarization) are located at the top of each antenna. The signals from the two LNAs are sent through two coaxial cables to small boxes, where the signals are amplitude-modulated and transmitted via Radio-Frequency-over-Fiber (RFoF). Each box supports 16 antennas and provides the antennas also with the necessary power. Sixteen boxes are needed to serve the 256 antennas in the station. Each station has got a different random layout, and the positioning of each box is arranged within the ground plane diameter to ensure a maximum length of the coaxial cable of about 10 m.

III. EM MODELLING

The results shown in this contribution are based on an EM analysis performed through the commercial Galileo-EMT package developed by IDS [2]. In order to perform a full-wave analysis including the mutual coupling effects among the antennas, which are quite strong due to the closeness of the antennas and the low frequencies involved, we have used the Method of Moment technique accelerated through MLFMA.

The full-station case is composed by 256 aluminum SKALA4.0 antennas randomly distributed according to the geometry of the Aperture Array Verification System 1 (AAVS1) scaled by a factor 38/35 to make the maximum center-to-center distance among antennas around 38 m [3]. The layout geometry is shown in Fig. 2. An accurate meshing of this model requires approximately 1 million degrees of freedom. While the reference antenna for the

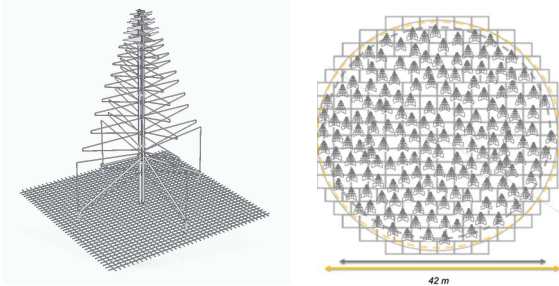


Fig. 1. (Left) SKALA4.0 antenna, physical dimension: 2.1 m height, 1.6 m maximum length. (Right) Example of an SKA1-Low station.

System CDR is the SKALA4.1, for this analysis we have used the model of the previous version of the SKALA antenna (4.0), whose EM model is 40% lighter than the new one. However, for the target of this contribution, the differences between the two antenna models are not expected to determine any significant impact on the effects of the ground plane and of the terrain.

Except for a very recent publication [4], most of the results presented so far on the SKA1-Low station performance are based on an infinite pec ground plane. This allows to use the reflection coefficient approximation adding a reflected component to the field, which is a very fast technique. However, as already stated the real ground plane will have a finite diameter, which determines a truncation of the electrical currents induced in the ground plane and diffraction effects. Moreover, especially the outer antennas will be affected by the presence of the terrain beyond the metallic ground plane. The terrain can be treated as dielectric medium with different electrical parameters for different humidity conditions.

In order to rigorously take into account the finiteness of the ground plane, this should be simulated through a full-wave technique. This approach would determine the currents on the antennas and on the plate considering their reciprocal interaction. However, this would lead to an extremely large linear problem. Therefore, for the purpose of this research, the problem has been addressed through a simplified 3-steps process, which consists of:

- A1. firstly, we compute the currents induced on the 256 antennas considering an infinite ground plane with reflection coefficient approximation;
- A2. then, starting from the currents of the previous point the currents induced on a finite ground plane are computed with a full-wave approach;
- A3. finally, the currents distributed in the antennas and in the finite ground plane are radiated applying the equivalence principle to obtain the scattered field.

Furthermore, the presence of different dielectric media beyond the ground plane is computed for a single antenna only, therefore without accounting for the coupling with the near antennas of the full-station. Here the following approach has been used:

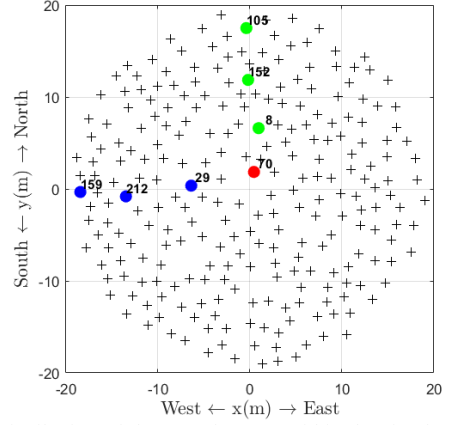


Fig. 2. Distribution of the 256 elements within the simulated station. The antennas highlighted in blue are used to estimate the effect of the finite ground plane on the H-plane, while the green antennas in the E-plane. The central red antenna is used for both planes.

- B1. firstly, we compute with a full-wave approach the currents induced on the antenna and on the plane considering a finite ground plane with air;
- B2. then, the currents distributed in the antenna and in the finite ground plane are radiated applying the equivalence principle and considering the different electrical properties of the dielectric beyond the ground plane.

It is worthwhile mentioning that in all cases listed above, the ground plane is always considered a solid pec plane.

IV. NUMERICAL RESULTS

The numerical results are divided in two sub-sections, one discussing the effects of the finite ground plane for different positions of the antennas in the array along the two principle planes according to the procedure indicated with A in section III. The other sub-section presents the effects of the dielectric terrain in addition to the ground plane (procedure B). The results of the first sub-section are shown in terms of Embedded Element Patterns (EEPs) with respect to the ideal infinite ground plane case; while for the second sub-section, the patterns of a single antenna are evaluated for different dielectric characteristics. Furthermore, the frequencies selected correspond to the edges of the nominal bandwidth of SKA1-Low (50 and 350 MHz) and with the excited port of the antennas aligned in the North-South direction. Due to the high symmetry of the antenna, we assume that very similar results can be obtained for the other orthogonal polarization.

A. Finite ground plane

It is reasonable expecting that the impact of the finite ground plane to the EEPs varies with the antenna distance from the ground edge. Therefore, we have selected one antenna close to the center plus three other antennas quite evenly distributed along two main directions, North-South

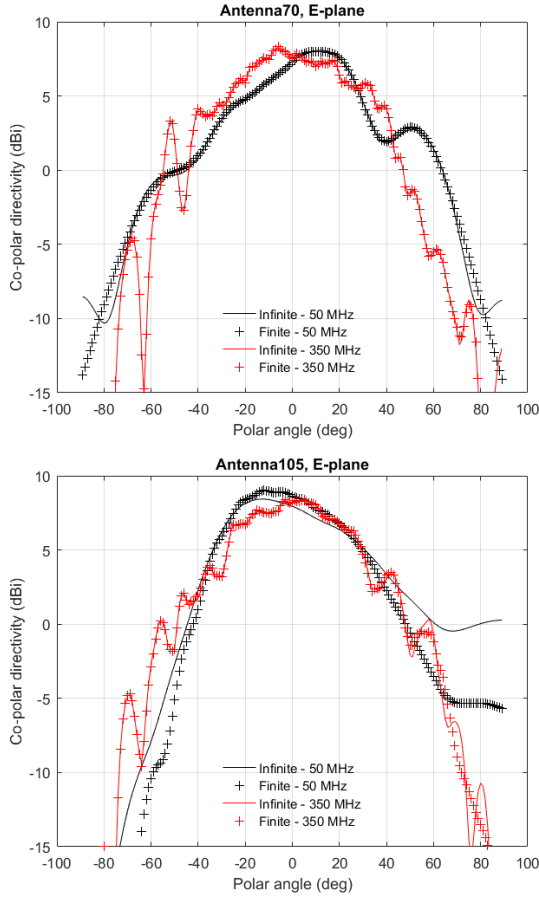


Fig. 3. E-plane directivity pattern with infinite (continue lines) and finite ground (cross markers) at 50 and 350 MHz (black and red respectively) for two antennas: central antenna (top plot) and outer antenna (bottom plot).

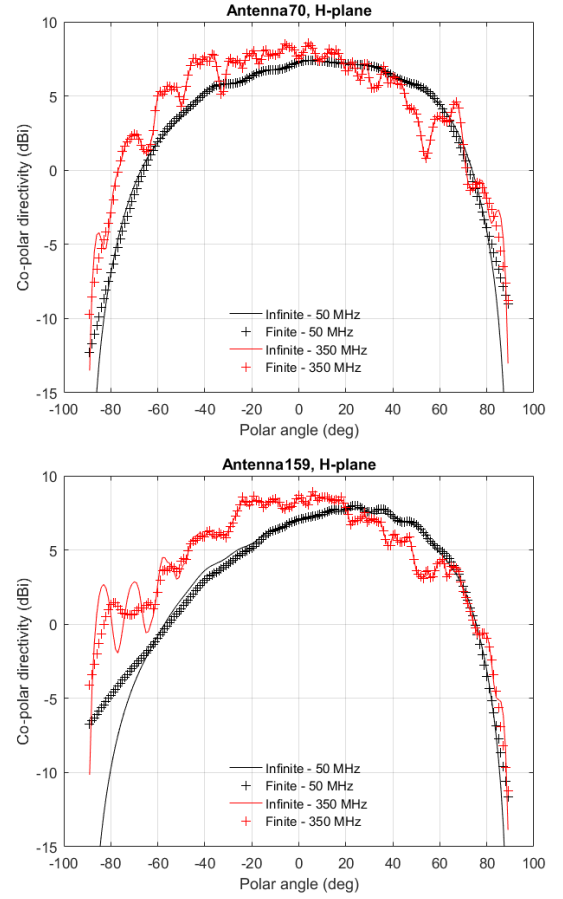


Fig. 4. H-plane directivity pattern with infinite (continue lines) and finite ground (cross markers) at 50 and 350 MHz (black and red respectively) for two antennas: central antenna (top plot) and outer antenna (bottom plot).

and East-West (see Fig. 2). In such way, for each plane, all the antennas see the edge with approximately a similar pattern and therefore only the distance from the edge contributes to the difference between considering an infinite and a finite plane. The finite plane case is composed by a circle with 42 m diameter and air beyond it.

For the E-plane and H-plane, Figs. 3 to 6 show the antenna directivity for the central antenna (#70) and the outer ones (#105 and #159 respectively). For the central antenna in both planes and both frequencies, the two computations (finite and infinite ground plane) provide almost identical directivities except for small differences at very low elevations. This is no longer true for the outer antennas, where some differences between the pair of curves appear also at very high elevation (see for instance E-plane at 50 MHz of antenna #105 in Fig. 3). Generally speaking, the differences in the patterns of the outer antennas between finite and infinite cases are higher at 50 MHz than at 350 MHz. This is likely due to the larger distribution of the electrical currents in the infinite ground plane at 50 MHz. At 350 MHz, the pattern obtained by the infinite ground plane shows more ripple at low elevation with respect to the finite

case. This could be explained by currents distributed in the infinite ground plane, which produce an in-phase or an opposite-phase contribution to the fields radiated by the antenna currents in different angular directions.

As a figure of merit of the agreement between the two cases, we choose the mean, in each principle plane, of the absolute values of the difference between the two patterns in a linear scale. This figure of merit, which is computed for all antennas highlighted in Fig. 2, confirms that, for both frequencies, the general trend is an increment of the discrepancy with the vicinity of the antennas to the edge (see Fig. 5). Moreover, the behavior at 50 MHz is more affected by the ground plane approximation than the one at 350 MHz. The current analysis emphasizes that while for some combinations of antenna/frequency/plane the ground plane approximation does not play a significant role, there are antennas where this effect cannot be neglected.

B. Dielectric terrain

The effects of the dielectric terrain on the pattern have been computed for the antenna #105, which is very close to

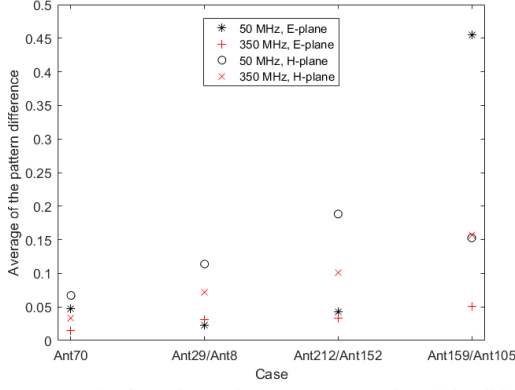


Fig. 5. Average in the polar angle range $[-89:89]$ deg of the difference between directivities computed with finite and infinite ground plane. Results are reported at 50 and 350 MHz for every antenna highlighted in Fig. 2 and grouped for similar distance from the center (for instance antennas #29 and #8 are 6.5 m far from the origin in the H- and E-plane respectively).

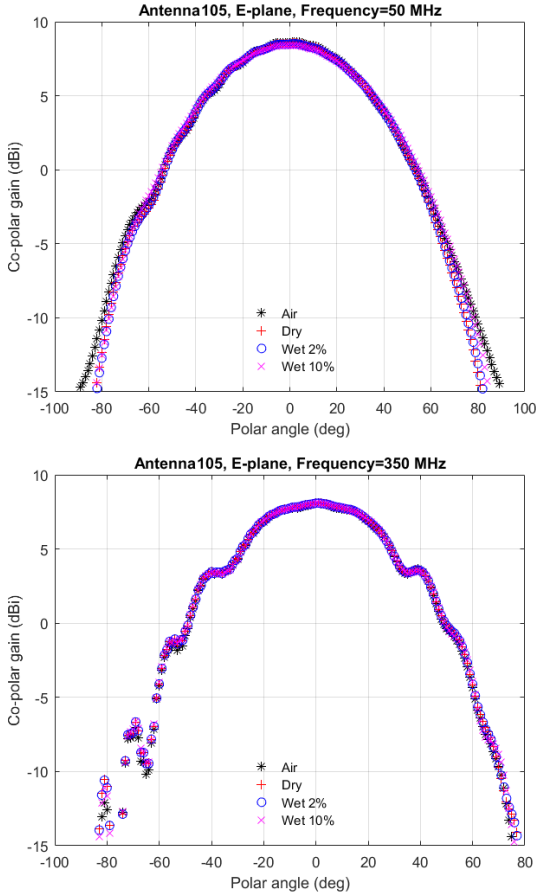


Fig. 6. E-plane gain pattern for the antenna #105, in isolated condition, with a finite ground and different dielectric (from air to wet terrain). The top plot is computed at 50 MHz, while the bottom one at 350 MHz.

the edge of the ground plane and, as shown in the previous section, is quite sensitive to the approximation done on the ground plane. This analysis has been conducted for the single

case, so without any antenna in the station, which determines a smoother behavior of the pattern than that computed with mutual coupling. This simplification is based on the assumption that the possible perturbation due to the medium surrounding the antenna under test should not be affected by the presence of the other antennas.

Four different media beyond the finite ground plane have been considered in the analysis, each of them characterized by different relative permittivity (ϵ) and electrical conductivity (σ , S/m) as reported in Table I [5].

The curves of Fig. 6 represent the antenna gains computed for different media filling the volume after the circular ground plane. At 50 and 350 MHz, the antenna gain behaviors are very similar regardless of the electrical characteristics of the dielectric. At 50 MHz, the radiation efficiency turns out to be above 98% for all the terrains analyzed, while the maximum gain decreases from 8.65 to 8.41 dBi (corresponding to a 5% reduction) if, instead of the air, the terrain with 10% moisture level is considered. On the other hand, at 350 MHz there are no differences in the antenna gain between lossless and loss dielectrics.

TABLE I. ELECTRICAL RELATIVE PERMITTIVITY AND CONDUCTIVITY FOR DIFFERENT MOISTURE LEVELS

Freq. (MHz)	Parameter	Terrain condition			
		Air	Dry	2%	10%
50	ϵ	1	3.9	6.5	17.8
	σ	0	7e-4	1e-2	1e-1
350	ϵ	1	3.7	4.6	14.2
	σ	0	2.4e-3	2.2e-2	1.1e-1

V. CONCLUSIONS

Our preliminary results show that, for one station of SKA1-Low, the implementation in numerical EM code of a finite ground plane leads to not negligible differences with respect to the infinite ground plane, especially for the antennas closer to the edge of the plane. This analysis has been also extended to different dielectric terrains. Variations in the electrical relative permittivity and conductivity do not significantly modify the antenna pattern, while the maximum gain can decrease by up to 5%.

Computational times with a workstation (2*Xeon E5-2697v4 @ 3.6GHz (36 cores) and 1 TB RAM) are reported in Table II. The analysis is very time-consuming when it comes to simulate a full SKA1-Low station including 256 antennas, as in step A1 of the finite ground plane case. A part for that, all other steps in the finite ground plane case and in the dielectric terrain case are solved with limited amount of time.

As a future activity, a statistics analysis of all the EEPs of a full-station could help in defining some general guidelines on the effects of the finiteness of the ground plane. For instance, it would be interesting to identify a distance from the edge, after which the antenna patterns are affected below a certain threshold by the ground plane approximation.

TABLE II. COMPUTATIONAL TIME (IN HOURS/MINUTES/SECONDS)
FOR THE SIMULATIONS PERFORMED FOLLOWING THE STEPS DESCRIBED IN
SECTION III.

<i>Finite ground plane case</i>			
Freq. (MHz)	A1	A2	A3
50	70 h	45 m	2 m
350	47 h	5 m	2 m
<i>Dielectric terrain case</i>			
Freq. (MHz)	B1	B2	-
50	10 m	1 s	-
350	15 m	21 s	-

ACKNOWLEDGMENT

This activity has been carried out in collaboration with the AAVS1.5 group constituted during the SKA Bridging phase.

REFERENCES

- [1] M. G. Labate, R. Braun, P. Dewdney, M. Waterson, J. Wagg, "SKA1-LOW: Design and scientific objectives," *XXXIInd GASS-URSI*, (Montreal, Canada), August 19-26, 2017.
- [2] <https://www.idscorporation.com/pf/galileo-suite/>
- [3] P. Di Ninni, M. Bercigli, P. Bolli, G. Virone, S.J. Wijnholds, "Mutual Coupling Analysis for a SKA1-LOW Station," *13th EUCAP*, (Krakow, Poland), 31 March – 5 April, 2019.
- [4] J. Cavillot, D. Tihon, C. Craeye, E. de Lera Acedo, N. Razavi-Ghods, "Fast simulation technique for antenna installed on a finite ground plane," *2019 ICEAA*, (Granada, Spain), September 9-13, 2019.
- [5] A. T. Sutinjo, et al., "Characterization of a Low-Frequency Radio Astronomy Prototype Array in Western Australia," *IEEE Transactions on Antennas and Propagation*, vol. 63, 12, December 2015.